PHYSICAL REVIEW B VOLUME 58, NUMBER 13 1 OCTOBER 1998-I

Nuclear resonant inelastic absorption of synchrotron radiation in an anisotropic single crystal

V. G. Kohn
Russian Research Centre ''Kurchatov Institute,'' 123182, Moscow, Russia

A. I. Chumakov and R. Rüffer
European Synchrotron Radiation Facility, Boîte Postal 220, F-38043 Grenoble, France

(Received 15 January 1998)

The Singwi and Sjölander theory of nuclear resonant inelastic absorption of x rays is extended to the general case of an anisotropic single crystal. The energy dependence of nuclear inelastic absorption for the specific direction of the x-ray quantum relative to the crystal lattice is described using the density of phonon states, weighted by the projection of the phonon polarization vectors to the wave vector of the x-ray quantum. An applicability of the sum rules in the case of the anisotropic crystal is analyzed. The method of calculation of the phonon projected density of states from experimental data is proposed, where deconvolution of the data with the instrumental function of the monochromator and the subtraction of the multiphonon absorption is handled using the Fourier transformation. The results are illustrated by processing the experimental data of nuclear inelastic absorption of x rays in the anisotropic ferric borate $FeBO_3$ single crystal. [S0163-1829(98)01938-9]

I. INTRODUCTION

Inelastic scattering of radiation with creation or annihilation of phonons is a powerful technique to study the lattice dynamics. Neutron,[1] x-ray,[2] and light[3] inelastic scattering have long been used to measure the phonon dispersion law $\omega(\mathbf{q})$, where $\hbar\omega$ is the phonon energy and $\mathbf{q}$ is the wave vector. Recent progress in the domain of nuclear resonant scattering of synchrotron radiation[4] paved the way for a new inelastic technique, nuclear inelastic absorption.[5] Measurements of nuclear inelastic absorption benefit much from the large nuclear resonant cross section, so the new field develops rapidly.[6–9] The theoretical description of nuclear inelastic absorption in the case of an isotropic crystal was done by Singwi and Sjölander[10] (for other relevant theoretical papers see Refs. 11,12).

The determination of phonon energy by means of nuclear inelastic absorption assumes no momentum resolved information on the phonon spectra and therefore is not applicable to the investigation of the phonon dispersion law $\omega(\mathbf{q})$. Instead of this, the experimental energy spectra of inelastic nuclear absorption are discussed in terms of the phonon density of states (DOS) $g(E)$. This is described by the Singwi and Sjölander theory,[10] which was proposed for a crystal with a cubic Bravais lattice. The theory fails to describe the anisotropy of nuclear inelastic absorption, which has been recently observed[9] in the $FeBO_3$ single crystal. Therefore a more general theoretical description is necessary, which takes into account the direction of the incident x-ray beam relative to the crystal lattice and considers the densities of phonon states with various phonon polarizations. Such a theory is the main subject of this work.

Another problem we address is the calculation of the phonon density of states from the experimental data. In order to extract the density of states, one has to deconvolute the data with the instrumental function of the monochromator and to separate the single-phonon absorption from the multiphonon contributions. The first problem may be partially overcome with an x-ray monochromator of higher energy resolution. However, even in this case the elimination of the instrumental function remains desirable. We show that both problems can be solved successfully using the forward and the reversed Fourier transformations of the data from energy to time space.

We illustrate the developed technique by two examples: nuclear inelastic absorption in the polycrystalline α-iron foil and anisotropic nuclear inelastic absorption in the ferric borate $FeBO_3$ single crystal. In the first case we demonstrate the reliability of the data processing technique by comparing the calculated DOS with the data known from a neutron scattering experiment.[13] In the second case we obtain the densities of states, weighted by the projection of the phonon polarization vectors to the different crystallographic axes. They significantly differ in shape, revealing the anisotropy of the lattice vibrations in the noncubic single crystal.

II. THE PROBABILITY OF NUCLEAR INELASTIC ABSORPTION OF X RAYS IN A SINGLE CRYSTAL

We start from the general expression for an x-ray absorption cross section per a nucleus in terms of the time integral, which was obtained by Singwi and Sjölander.[10] We assume that the phonon energy is much larger than the possible hyperfine splitting of the nuclear levels, therefore the hyperfine structure can be neglected. In contrast to Ref. 10 we consider in the explicit form a crystal with a complex unit cell, which may contain several different atoms as well as several identical atoms at various positions. Let the total number of resonant nuclei per unit cell be n_r. The resonant nuclei in the unit cell are labeled with index m. We consider the normalized probability of absorption $W(E)$ per unit energy interval at the energy E. Now Eq. (2) of Ref. 10 can be rewritten as follows:

$$W(E)=\int\frac{d\tau}{2\pi}\exp\left(-iE\tau-\frac{\Gamma}{2}|\tau|\right)\frac{1}{n_r}\sum_m F_m(\mathbf{k},\tau), \quad (1)$$

where $\tau = t/\hbar$, t is the time, Γ is the natural width of the nuclear excited state, E is the energy of the x-ray quantum relative to the resonance energy of nuclear transition, and $\mathbf{k}$ is the wave vector of the incident γ ray. The function

$$F_m(\mathbf{k},\tau) = \langle \exp[-i\mathbf{k}\mathbf{u}_m(0)]\exp[i\mathbf{k}\mathbf{u}_m(\tau)]\rangle \tag{2}$$

is the time-dependent correlation function, which describes the correlation between the displacements $\mathbf{u}_m$ of the nucleus at two different moments of time separated by the time interval $t = \hbar\tau$. In the single crystal this function has translational symmetry. It may be different for various nuclei inside the unit cell.

To deal with this function, Singwi and Sjölander[10] introduced the Van Hove space-time correlation function $G_s(\mathbf{r},t)$ in a spherically symmetrical approximation. Afterwards they applied this function to the case of a cubic Bravais lattice. In this way the dependence on the direction of the photon beam has been lost. However, it is not necessary to consider the space-time correlation function $G_s(\mathbf{r},t)$ for the calculation of $F_m(\mathbf{k},\tau)$. As it was shown by Van Hove [see Eq. (51) of Ref. 14], this function can be represented in a general case of an anisotropic crystal as follows:

$$F_m(\mathbf{k},\tau) = \exp[-Z_m(\mathbf{k})]\exp[M_m(\mathbf{k},\tau)], \tag{3}$$

where

$$Z_m(\mathbf{k}) = M_m(\mathbf{k},0) = \frac{E_R}{N}\sum_{\mathbf{q}j} \frac{|\mathbf{s}\cdot\mathbf{e}_{mj}(\mathbf{q})|^2}{\hbar\omega_j(\mathbf{q})}(2\bar{n}_{\mathbf{q}j}+1), \tag{4}$$

$$M_m(\mathbf{k},\tau) = \frac{E_R}{N}\sum_{\mathbf{q}j} \frac{|\mathbf{s}\cdot\mathbf{e}_{mj}(\mathbf{q})|^2}{\hbar\omega_j(\mathbf{q})}\{(\bar{n}_{\mathbf{q}j}+1)\exp[i\hbar\omega_j(\mathbf{q})\tau] + \bar{n}_{\mathbf{q}j}\exp[-i\hbar\omega_j(\mathbf{q})\,\tau]\}. \tag{5}$$

Equations (3)–(5) extend the Van Hove formulas to the general case of a non-Bravais crystal lattice with several resonant nuclei in the unit cell. The derivation is similar to that given by Van Hove[14] and we omit it here. In the formulas (4),(5) $E_R = \hbar^2k^2/2M$ is the recoil energy, N is the number of unit cells per unit volume of a crystal, $\omega_j(\mathbf{q})$ is the phonon dispersion relation for the branch j, $\mathbf{e}_{mj}(\mathbf{q})$ is the polarization vector of vibrations for mth atom in the mode $\{\mathbf{q}j\}$, $\mathbf{s} = \mathbf{k}/k$,

$$\bar{n}_{\mathbf{q}j} = \{\exp[\beta\hbar\omega_j(\mathbf{q})]-1\}^{-1} \tag{6}$$

is the Bose-Einstein distribution function, $\beta = (k_BT)^{-1}$, k_B is the Boltzmann constant, and T is the temperature. We note that $\exp[-Z_m(\mathbf{k})] \equiv f_m(\mathbf{k})$ is the angular-dependent Lamb-Mössbauer factor.

To calculate the integral in Eq. (1) we expand the exponent $\exp[M_m(\mathbf{k},\tau)]$ in powers series of the argument and arrive at the expansion $W(E) = \Sigma_{n=0}^{\infty} W_n(E)$, where each term corresponds to the photon absorption accompanied by creation or annihilation of n phonons.

The zero term of this expansion describes elastic nuclear absorption, which is not accompanied by phonon creation or annihilation. It can be calculated directly using the tabulated integral

$$\int \frac{d\tau}{2\pi}\exp\left(-iE\tau - \frac{\Gamma}{2}|\tau|\right) = \frac{1}{2\pi}\,\frac{\Gamma}{(E^2+\Gamma^2/4)} = \delta_\Gamma(E). \tag{7}$$

As a result we have

$$W_0(E) = \delta_\Gamma(E)\frac{1}{n_r}\sum_m f_m(\mathbf{k}), \qquad \lim_{\Gamma\to 0}\delta_\Gamma(E) = \delta(E), \tag{8}$$

where $\delta(E)$ is the Dirac δ function.

The first term describes the single-phonon nuclear inelastic absorption. It is calculated through the same integral (7), however, the result has a more complicated form:

$$W_1(E) = \frac{E_R}{Nn_r}\sum_m f_m(\mathbf{k})\sum_{\mathbf{q}j}\frac{|\mathbf{s}\cdot\mathbf{e}_{mj}(\mathbf{q})|^2}{\hbar\omega_j(\mathbf{q})}\{(\bar{n}_{\mathbf{q}j}+1)\delta_\Gamma \times[E-\hbar\omega_j(\mathbf{q})] + \bar{n}_{\mathbf{q}j}\delta_\Gamma[E+\hbar\omega_j(\mathbf{q})]\}. \tag{9}$$

After the replacement of $\delta_\Gamma(E)$ by $\delta(E)$ and taking into account that $\bar{n}_{\mathbf{q}j}$ depends only on $\hbar\omega_j(\mathbf{q})$ [see Eq. (6)], the expression (9) can be represented as follows:

$$W_1(E) = \frac{1}{n_r}\sum_m f_m(\mathbf{k})\,S_m^{(1)}(E,\mathbf{k}),$$

$$S_m^{(1)}(E,\mathbf{k}) = \frac{E_R\,g_m(|E|,\mathbf{s})}{E[1-\exp(-\beta E)]}. \tag{10}$$

The form of this expression is similar to that used for the polycrystalline sample (see, for example, Refs. 6,7). However, the dependence of the absorption probability on the direction of the incident photon beam relative to the crystal lattice is obtained here in an explicit form through the function

$$g_m(E,\mathbf{s}) = V_0\sum_j\int\frac{d\mathbf{q}}{(2\pi)^3}\delta[E-\hbar\omega_j(\mathbf{q})]|\mathbf{s}\cdot\mathbf{e}_{mj}(\mathbf{q})|^2 = \frac{V_0}{(2\pi)^3}\sum_j\int\frac{dq_1dq_2}{|\mathrm{grad}_{\mathbf{q}}\hbar\omega_j(\mathbf{q})|}|\mathbf{s}\cdot\mathbf{e}_{mj}(\mathbf{q})|^2. \tag{11}$$

Here $V_0 = 1/N$ is the volume of the unit cell. We have passed from the sum to the integral according to the usual technique. The integral is taken over the surface of the constant energy $\hbar\omega_j(\mathbf{q}) = E$ in $\mathbf{q}$ space within the first Brillouin zone. The coordinates q_1 and q_2 are the axes of the local reference Cartesian system. They lie on the surface of the constant energy E. The third axis q_3 of Cartesian system is directed along the vector $\mathrm{grad}_{\mathbf{q}}\hbar\omega_j(\mathbf{q})$.

The function $g_m(E,\mathbf{s})$ coincides with the conventional phonon density of states for an isotropic crystal, where $\omega_j(\mathbf{q})$ does not depend on j. Taking into account the property of the polarization vectors $\Sigma_j|\mathbf{s}\cdot\mathbf{e}_{mj}(\mathbf{q})|^2 = 1$ we find that the dependence on $\mathbf{s}$ vanishes in this case. The dependence on $\mathbf{s}$ also vanishes for a polycrystalline sample, where the direction of photon beam relative to the crystal lattice averages over many crystalline grains. However, in an anisotropic single crystal the function $g_m(E,\mathbf{s})$ does not coincide with the DOS. In contrast to the DOS, it contains the contributions of phonons, weighted by the projection of their polarization vectors to the direction of the x-ray beam.

Therefore we will call this function the projected density of states (PDOS). We note that it may be different for various sites m of the resonant nuclei in the unit cell. As will be shown below, this function is normalized to unity for any $\mathbf{s}$ direction.

Considering the higher-order terms of the multiphonon expansion we omit the energy width Γ of the nuclear levels as negligible compared to the phonon energy. Then we rewrite Eq. (1) as follows:

$$W_n(E)=\frac{1}{n_r}\sum_m f_m(\mathbf{k})\,S_m^{(n)}(E,\mathbf{k}), \tag{12}$$

where

$$S_m^{(n)}(E,\mathbf{k})=\int\frac{d\tau}{2\pi}\exp(-iE\tau)\frac{M_m(\mathbf{k},\tau)}{n}\,\frac{[M_m(\mathbf{k},\tau)]^{n-1}}{(n-1)!}. \tag{13}$$

The integral in Eq. (13) is the Fourier image of the product of two functions. It can be represented as the convolution of the Fourier images of these functions. This leads to the recursive relation

$$S_m^{(n)}(E,\mathbf{k})=\frac{1}{n}\int dE'\,S_m^{(1)}(E',\mathbf{k})\,S_m^{(n-1)}(E-E',\mathbf{k}), \tag{14}$$

which permits us to calculate the multiphonon scattering cross section from the single-phonon term.

As a result we obtain the expression for the probability of nuclear absorption in a form which is similar to the formula obtained by Singwi and Sjölander,[10] namely,

$$W(E,\mathbf{k})=\frac{1}{n_r}\sum_m f_m\left(\delta_\Gamma(E)+\sum_{n=1}^{\infty}S_m^{(n)}(E,\mathbf{k})\right). \tag{15}$$

In our case, however, the explicit dependence of nuclear absorption on the direction $\mathbf{k}$ of the photon propagation relative to the crystal lattice is revealed through the projected density of phonon state $g_m(E,\mathbf{s})$.

In order to calculate the Lamb-Mössbauer factor we note that

$$S_m^{(1)}(E,\mathbf{k})=\int\frac{d\tau}{2\pi}\exp(-iE\tau)\,M_m(\mathbf{k},\tau), \tag{16}$$

therefore

$$M_m(\mathbf{k},\tau)=\int dE\,\exp(iE\tau)\,S_m^{(1)}(E,\mathbf{k}). \tag{17}$$

Now from Eqs. (4) and (10) we obtain the Lamb-Mössbauer factor

$$f_m(\mathbf{k})=\exp\left(-E_R\int_0^{\infty}dE\,g_m(E,\mathbf{s})\,E^{-1}\frac{1+\exp(-\beta E)}{1-\exp(-\beta E)}\right). \tag{18}$$

We see that the Lamb-Mössbauer factor in an anisotropic crystal is determined completely by PDOS.

III. LIPKIN SUM RULES

The Lipkin sum rules[12] offer a useful tool for treating the data on inelastic nuclear absorption, because they simplify the normalization of the experimental spectra.[6] Therefore it is important to investigate the application of the sum rules in the case of an anisotropic single crystal. We rewrite Eq. (1) as follows:

$$\begin{aligned}W(E)&=\int\frac{d\tau}{2\pi}\exp(-iE\tau)\Phi(\tau)\\&=\frac{1}{E^n}\int\frac{d\tau}{2\pi}\exp(-iE\tau)\left(\frac{d^n\Phi(\tau)}{i^n d\tau^n}\right),\end{aligned} \tag{19}$$

where

$$\Phi(\tau)=\exp\left(-\frac{\Gamma}{2}|\tau|\right)\frac{1}{n_r}\sum_m F_m(\mathbf{k},\tau) \tag{20}$$

is the Fourier image of the energy spectrum of the absorption probability. The right side of Eq. (19) is obtained by integration by parts taking into account that $\Phi(\tau)$ and all its derivatives equal zero at $|\tau|\rightarrow\infty$.

We will use the notation $\langle E^n\rangle_A=\int_{-\infty}^{\infty}dE\,A(E)\,E^n$ for the nth momentum of the function $A(E)$. The zero momentum of the absorption probability is

$$\langle E^0\rangle_W=\int dE\,W(E)=\Phi(0)=1, \tag{21}$$

which follows immediately from the left side of Eq. (19) and the expression (3). This proves the correct normalization of the absorption probability in Eq. (1).

The first momentum can be easily calculated through the right side of Eq. (19) with $n=1$, namely,

$$\begin{aligned}\langle E^1\rangle_W&=\int dE\,W(E)\,E=\left(\frac{d\Phi(\tau)}{id\tau}\right)_{\tau=0}\\&=\frac{1}{n_r}\sum_m\left(\frac{dM_m(\mathbf{k},\tau)}{id\tau}\right)_{\tau=0}.\end{aligned} \tag{22}$$

Substitution of Eq. (5) gives

$$\begin{aligned}\langle E^1\rangle_W&=\frac{E_R}{Nn_r}\sum_{m\mathbf{q}j}\frac{|\mathbf{s}\cdot\mathbf{e}_{mj}(\mathbf{q})|^2}{i\hbar\omega_j(\mathbf{q})}\\&\quad\times[i\hbar\omega_j(\mathbf{q})\,(\overline{n}_{\mathbf{q}j}+1)-i\hbar\omega_j(\mathbf{q})\overline{n}_{\mathbf{q}j}]\\&=\frac{E_R}{Nn_r}\sum_{m\mathbf{q}j}|\mathbf{s}\cdot\mathbf{e}_{mj}(\mathbf{q})|^2=E_R.\end{aligned} \tag{23}$$

Thus we obtain the Lipkin sum rule:[12] the first momentum of the total probability of nuclear absorption equals the mean recoil energy E_R.

The higher-order energy momenta can be calculated similarly. For example, the second energy momentum of the absorption probability equals

$$\langle E^2\rangle_W=\int dE\,W(E)\,E^2=\left(-\frac{d^2\Phi(\tau)}{d\tau^2}\right)_{\tau=0}. \tag{24}$$

We note that this momentum diverges if the integral is taken over the infinite energy interval. The divergence results from the property of the function $\delta_\Gamma(E)$, which is not exactly the δ function, but behaves as E^{-2} at the tails. However, in practice we handle the data, which are taken over the finite energy range of $2E_{\max}$, where $E_{\max}$ is larger than the phonon energy but much smaller than $\langle E^2\rangle/\Gamma$. This allows us to neglect the tails during the integration and treat $\delta_\Gamma(E)$ as the exact δ function for all considered energies. In this approximation we obtain

$$\begin{aligned}\langle E^2\rangle_W &= E_R^2 + \frac{E_R}{Nn_r}\sum_{m\mathbf{q}j} |\mathbf{s}\cdot\mathbf{e}_{mj}(\mathbf{q})|^2\,\hbar\omega_j(\mathbf{q})\,(2\overline{n}_{\mathbf{q}j}+1)\\ &= E_R^2 + E_R\frac{1}{n_r}\sum_m \int_0^\infty dE\, g_m(E,\mathbf{s})\, E\,\frac{1+\exp(-\beta E)}{1-\exp(-\beta E)}.\end{aligned} \tag{25}$$

To obtain this expression we multiplied the right-hand side by unity in the form $\int_0^\infty dE\ \delta[E-\hbar\omega_j(\mathbf{q})]$ and performed the integration.

Using the same approximation one may consider the higher energy momenta. For example,

$$\langle E^3\rangle_W = E_R^3 + \frac{1}{n_r}\sum_m \int_0^\infty dE\, g_m(E,\mathbf{s}) \times\left(3E_R^2 E\,\frac{1+\exp(-\beta E)}{1-\exp(-\beta E)} + E_R E^2\right). \tag{26}$$

The theory presented above describes *incoherent* nuclear absorption, which is valid only for the *inelastic* contribution. Due to the relatively small cross section of inelastic absorption the experimental data in this case are proportional to the absorption probability. In contrast to that, *elastic* interaction of x rays with nuclei may also proceed *coherently*. In this case the x-ray field in the sample is governed by forward scattering,[15] which significantly influences the absorption process. The signal, which is measured in the experiment (delayed fluorescence radiation), is no longer proportional to the absorption probability. It can be described by the more extended theory.[16] Therefore the experimental energy spectra of nuclear absorption do not provide the correct ratio of elastic and inelastic contributions. Thus it is of interest to consider the energy momenta separately for the elastic and inelastic parts of the absorption probability.

We note that the probability of elastic nuclear absorption $W_0(E)$ as determined by Eq. (8), leads to the zero momentum $\langle E^0\rangle_{W_0} = n_r^{-1}\Sigma_m f_m(\mathbf{k})$, whereas all other momenta equal zero. Therefore, the relations (23), (25), (26) hold for the inelastic part of nuclear absorption $W(E)-W_0(E)$ as well.

IV. CALCULATION OF PHONON PDOS

In this section we address the practical point of the calculation of the projected density of phonon states from the experimental data. PDOS can be obtained from the single-phonon term of inelastic absorption. Therefore this term has to be separated from elastic and multiphonon contributions. In addition, the experimental data are influenced by the finite energy bandwidth of the x-ray beam, whereas in the discussion above we assumed monochromatic radiation. Therefore it is necessary to examine the application of the Lipkin sum rules to the experimental energy spectra and to consider the deconvolution of the data with the instrumental function.

We note that the conventional measurements of inelastic absorption[5–9] do not allow one to distinguish the different sites of the resonant atoms in the unit cell. Therefore in the discussion below we omit the index *m*. By these means we obtain the density of phonon states, which is averaged over the different sites of the resonant atoms.

Let $P(E)$ be the normalized energy distribution of the quanta in the x-ray beam (instrumental function of the monochromator). We exclude the elastic part of the absorption from our analysis for the reasons discussed in the previous section, and consider only the inelastic part of the absorption. The experimental energy spectrum $I(E,\mathbf{k})$ can be represented as follows:

$$\begin{aligned}I(E,\mathbf{k}) &= I_0\int dE'\,P(E')\,W_{\mathrm{inel}}(E-E',\mathbf{k})\\ &= I_0 f_{\mathrm{LM}}(\mathbf{k})\int\frac{d\tau}{2\pi}\exp\left(-iE\tau-\frac{\Gamma}{2}|\tau|\right)Q(\tau)\\ &\quad\times\{\exp[M(\mathbf{k},\tau)-1]\}.\end{aligned} \tag{27}$$

Here I_0 is the scaling factor and $Q(\tau)$ is the Fourier image of $P(E)$. It is evident that $Q(\tau)$ is a peak with a characteristic width w which satisfies the inequality $w \gg \Gamma$. For example, if $P(E)$ is the Gaussian with the standard deviation [random mean square (RMS)] σ, then $Q(\tau)$ is also Gaussian with the RMS σ^{-1}:

$$P(E) = \frac{1}{\sigma\sqrt{2\pi}}\exp\left(-\frac{E^2}{2\sigma^2}\right),$$

$$Q(\tau) = \int dE\,\exp(iE\tau)P(E) = \exp\left(-\frac{\tau^2}{2\sigma^{-2}}\right). \tag{28}$$

Therefore we again may consider the limit $\Gamma\rightarrow 0$ and omit the term containing Γ.

The contribution of single-phonon absorption to the experimental data is

$$I_1(E,\mathbf{k}) = I_0\, f_{\mathrm{LM}}\,(\mathbf{k})\int dE'\,P(E')\,S_1(E-E',\mathbf{k}),$$

$$S_1(E,\mathbf{k}) = \frac{E_R\, g(|E|,\mathbf{s})}{E[1-\exp(-\beta E)]}. \tag{29}$$

We suppose that the function $E^{-1}[1-\exp(-\beta E)]^{-1}$ is slow in the range of the energy width of the monochromator. This leads to an approximate formula

$$I_1(E,\mathbf{k}) = I_0\, f_{\mathrm{LM}}\,(\mathbf{k})\,\frac{E_R\,\overline{g}(|E|,\mathbf{s})}{E[1-\exp(-\beta E)]}, \tag{30}$$

where

$$\begin{aligned}\overline{g}(E,\mathbf{s})&=\int dE'\,P(E')\,g(E-E',\mathbf{s})\\&=V_0\sum_j\int\frac{d\mathbf{q}}{(2\pi)^3}P[E-\hbar\omega_j(\mathbf{q})]|\mathbf{s}\cdot\mathbf{e}_{mj}(\mathbf{q})|^2.\end{aligned}\tag{31}$$

This function is the smoothed PDOS, where the δ function is replaced by the energy spectrum of the monochromator. This smoothing may be destructive because the function $g(E,\mathbf{s})$ is not a slow function in general. It may contain sharp peaks if the phonon dispersion branches have plane areas on the curve $\omega_j(\mathbf{q})$ in $\mathbf{q}$ space with a small value of $|\mathrm{grad}_{\mathbf{q}}\hbar\omega_j(\mathbf{q})|$. In this cases the deconvolution procedures are desirable.

Considering the higher-order terms, we note that the recursive relation (14), which was obtained for the multiphonon contributions to the absorption probability $S^{(n)}(E,\mathbf{k})$, is not valid for $I_n(E,\mathbf{k})$. Therefore the procedures which use the recursive relation (14) in order to eliminate the multiphonon terms from the experimental data are, in general, not exact. Here we propose a quite different approach, which allows one to separate the single-phonon term from multiphonon contributions simultaneously with the deconvolution of the data with the instrumental function.

In the first step we determine the scaling factor I_0. Similar to Ref. 6, we use for this purpose the sum rules. The zero and the first momentum of the experimental energy spectrum can be found as follows:

$$\langle E^0\rangle_I=\int dE\,I(E,\mathbf{k})=I_0[1-f_{\mathrm{LM}}(\mathbf{k})],\tag{32}$$

$$\langle E^1\rangle_I=\int dE\,I(E,\mathbf{k})\,E=\langle E^0\rangle_I\langle E^1\rangle_P+I_0\,E_R.\tag{33}$$

Here we use that $\langle E^0\rangle_P=Q(0)=\int dE\,P(E)=1$, because the instrumental function is normalized. It, however, can be asymmetric, therefore the first moment of $P(E)$ may be different than zero. From Eqs. (32), (33) we obtain I_0 and $f_{\mathrm{LM}}(\mathbf{k})$ as

$$I_0=(\langle E^1\rangle_I-\langle E^0\rangle_I\langle E^1\rangle_P)/E_R,\quad f_{\mathrm{LM}}(\mathbf{k})=1-\langle E^0\rangle_I/I_0.\tag{34}$$

In the next step we calculate the function $M(\mathbf{k},\tau)$ directly from the experimental energy spectrum using the Fourier transformation as follows:

$$M(\mathbf{k},\tau)=\ln[1+J(\mathbf{k},\tau)],\tag{35}$$

$$J(\mathbf{k},\tau)=\frac{\int dE\,\exp(iE\tau)\,I(E,\mathbf{k})}{I_0 f_{\mathrm{LM}}(\mathbf{k})Q(\tau)}.\tag{36}$$

Finally, we perform the reverse Fourier transformation and obtain the projected density of phonon states as

$$\begin{gathered}D(E,\mathbf{s})=\frac{E}{E_R}[1-\exp(-\beta E)]\int\frac{d\tau}{2\pi}\exp(-iE\tau)\,M(\mathbf{k},\tau),\\g(E,\mathbf{s})=D(|E|,\mathbf{s}).\end{gathered}\tag{37}$$

We note that Eq. (35) eliminates the multiphonon processes by means of logarithm function,[17] whereas Eq. (36) provides the deconvolution of the data with the instrumental function.

In addition, we consider the possibilities to verify the reliability of the experimental data and to check the procedure of their treatment. For this purpose we derive several relations, which connect the various energy momenta of the experimental data with those of PDOS. It is convenient to write them as the conditions on the function

$$G_n(\mathbf{s})=\int_0^\infty dE\,g(E,\mathbf{s})E^n\frac{1+C_n(E)}{1-C_n(E)},$$

$$C_n(E)=\frac{1-(-1)^n}{2}\exp(-\beta E).\tag{38}$$

From Eqs. (18), (23), (25), and (26) we obtain

$$G_{-1}(\mathbf{s})=\frac{1}{E_R}\ln\left(\frac{1}{f_{\mathrm{LM}}(\mathbf{k})}\right),\tag{39}$$

$$G_0(\mathbf{s})=1,\tag{40}$$

$$G_1(\mathbf{s})=E_R^{-1}\langle E^2\rangle_W-E_R,\tag{41}$$

$$G_2(\mathbf{s})=E_R^{-1}\langle E^3\rangle_W-3\langle E^2\rangle_W+2E_R^2,\tag{42}$$

where the momenta of probability density are connected with the measured data as follows:

$$\langle E^2\rangle_W=I_0^{-1}(\langle E^2\rangle_I-\langle E^2\rangle_P\langle E^0\rangle_I)-2\langle E^1\rangle_P E_R,\tag{43}$$

$$\begin{aligned}\langle E^3\rangle_W=I_0^{-1}(\langle E^3\rangle_I-\langle E^3\rangle_P\langle E^0\rangle_I)-3\langle E^1\rangle_P\langle E^2\rangle_W\\-3\langle E^2\rangle_P E_R.\end{aligned}\tag{44}$$

These relations follow directly from Eqs. (34)–(37).

Conditions (39)–(42) can be used for the verification of the experimental results. In particular, Eq. (39) gives the comparison of the Lamb-Mössbauer factor obtained from the area of the inelastic part of the normalized experimental energy spectrum to that calculated from the derived PDOS. Equation (40) verifies the normalization of PDOS.

Another possibility to examine the reliability of the experimental data is to compare the results of Eq. (37) for positive and negative values of E. The part of $E>0$ describes the PDOS, which is determined from the processes of phonon absorption, while the part of $E<0$ describes the PDOS from the processes of phonon creation. Both functions must coincide, namely, $D(-E,\mathbf{s})=D(E,\mathbf{s})$. In fact, it is more accurate to calculate the projected density of phonon states from the positive part, because the processes of phonon absorption provide higher statistical accuracy.

V. SINGLE-PHONON SCATTERING WITH SMALL ENERGY TRANSFER

The experimental energy spectra of nuclear inelastic absorption allows one to obtain the PDOS and the Lamb-Mössbauer factor. PDOS may be used to verify theoretical models of the dispersion relations and of the interatomic potential. The most simple analysis can be performed for small energy transfer, where only the acoustic phonons participate in the inelastic absorption. Let us estimate $g(E,\mathbf{s})$ in this limit.

For the acoustic modes $\omega_j(\mathbf{q})=qc_j(\mathbf{n})$, where $\mathbf{n}=\mathbf{q}/q$ is the unit vector along $\mathbf{q}$ and $c_j(\mathbf{n})$ is the sound velocity for the given direction of the phonon propagation. Using the spherical coordinates in the integral over $\mathbf{q}$ and calculating the integral over modulus q by means of the δ function we obtain

$$g(E,\mathbf{s})=E^2\frac{V_0}{(2\pi\hbar)^3}\int_0^{2\pi}d\varphi\int_0^{\pi}d\theta\sin\theta\sum_j\frac{|\mathbf{s}\cdot\mathbf{e}_j(\theta,\varphi)|^2}{c_j^3(\theta,\varphi)}$$

$$=E^2\frac{V_0}{2\pi^2\hbar^3}\frac{1}{\overline{c_s^3}(\mathbf{s})}. \tag{45}$$

Here we introduced the mean sound velocity $\overline{c_s}$ along the direction $\mathbf{s}$ through the relation

$$\overline{c_s}(\mathbf{s})=\left(\frac{1}{4\pi}\int_0^{2\pi}d\varphi\int_0^{\pi}d\theta\sin\theta\sum_j\frac{|\mathbf{s}\cdot\mathbf{e}_j(\theta,\varphi)|^2}{c_j^3(\theta,\varphi)}\right)^{-1/3}. \tag{46}$$

Equations (10) and (45) show, that for small energy transfer the probability of single-phonon absorption is approximately a linear function of energy:

$$\lim_{|E|\to 0}W_1(E,\mathbf{s})\approx f_{\mathrm{LM}}(\mathbf{s})\frac{E_R}{\beta}\frac{V_0}{2\pi^2\hbar^3}\frac{1}{\overline{c_s^3}(\mathbf{s})}\left(1-\frac{\beta}{2}E\right). \tag{47}$$

This function varies slowly with energy, so it is not influenced much by the convolution with the instrumental function. In the cases of negligible multiphonon processes Eq. (47) provides a useful approximation of the energy spectrum of inelastic absorption in the small energy region. This approximation helps to eliminate the central elastic peak from the experimental data. On the other hand, Eq. (45) allows one to estimate the mean velocity of sound for the particular crystallographic direction from the calculated PDOS.

VI. SPECIFIC EXAMPLES

In order to illustrate the theory we present here the examples of processing the experimental data for the polycrystalline α-iron foil and for the $\mathrm{FeBO_3}$ single crystal. As discussed above, in the case of polycrystalline α-iron [Fig. 1(a)] there is no dependence of nuclear absorption on the direction of the incident photon beam. Nevertheless we choose this example in order to demonstrate the reliability of the data processing, since the data on the phonon DOS of α-iron are available[13] from neutron scattering. For the $\mathrm{FeBO_3}$ single crystal we consider the energy spectra of nuclear absorption for two different orientation of the incident x-ray beam relative to the crystal lattice. One spectrum [Fig. 1(b)] was measured when the angle between the beam and the [111] axis was 85°, in the second case [Fig. 1(c)] the beam was parallel to the [111] axes (see Ref. 9 for the details of the crystal orientation). The data were taken at the Nuclear Resonance beamline[18] ID18 at the European Synchrotron Radiation Facility. The energy resolution of the monochromator[19] was 1.65 meV. The abundance of the resonant ^{57}Fe isotope in both samples was about 0.95. All data were taken at room temperature. The instrumental function of the monochromator $P(E)$ was known from the energy spectrum of forward scattering.

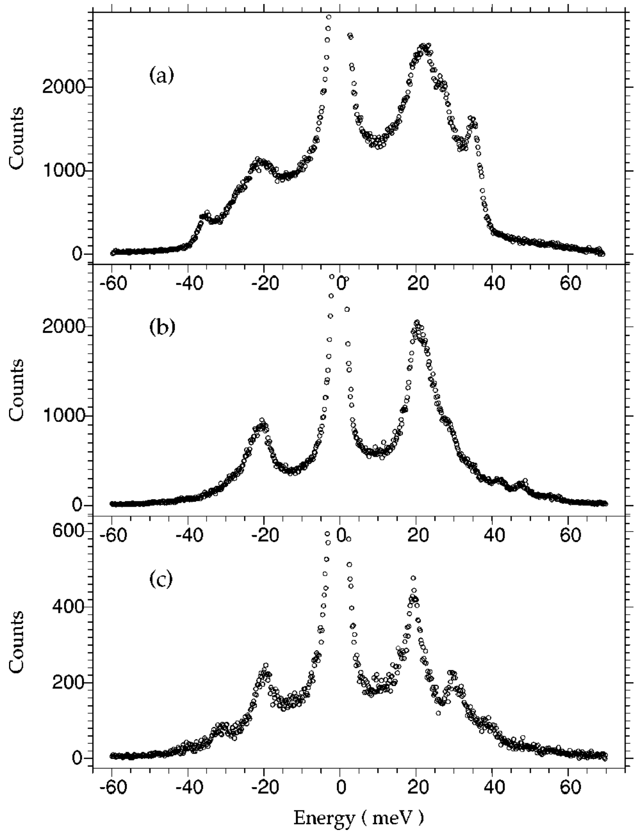

FIG. 1. Energy spectra of nuclear resonant absorption of synchrotron radiation (a) in the polycrystalline α-iron foil and (b),(c) in the $^{57}\mathrm{FeBO_3}$ single crystal, where the angle between the x-ray beam and the [111] axes was (b) 85° and (c) 0°.

In order to use the fast Fourier transformation code the experimental data were smoothed with use of the standard mathematical technique. This allowed us to decrease the statistical errors and to obtain the constant step array. The central peak of elastic absorption was removed from the experimental spectrum $I_{\mathrm{tot}}(E)$ according to the relation $I(E)=I_{\mathrm{tot}}(E)-\alpha P(E)$, where $I(E)$ stands for the energy spectrum of pure inelastic absorption. At room temperature the contribution of the multiphonon processes is small, therefore according to Eq. (47) $I(E)$ should be approximately linear in the vicinity of the central peak. This property was used to determine the factor α before the subtracted instrumental function. Then the derived energy spectrum of pure inelastic absorption $I(E)$ was normalized according to Eq. (34).

The density of the phonon states was calculated from the normalized spectrum of inelastic absorption through the for-

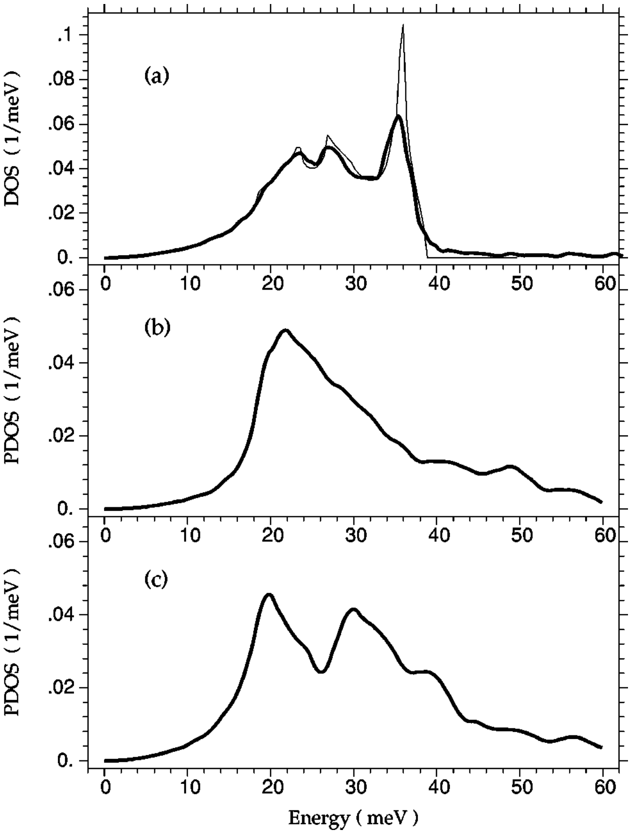

FIG. 2. Results of processing the experimental data from Fig. 1. (a) DOS for the polycrystalline α-iron foil, (b),(c) PDOS for the ^{57}FeBO$_3$ single crystal in the cases where the axis of projection has the angle of (b) 85° relative to the [111] axes, or (c) parallel to the [111] axes.

ward and the reversed Fourier transformations according to Eqs. (36) and (37). In practice, the complete deconvolution of the experimental data with the instrumental function is impossible, because it would increase significantly the remained statistical error of the data. Therefore applying Eq. (36) we used the function $(1+b)/[Q(\tau)+b]$ instead of $1/Q(\tau)$. This substitution means that the calculated function is not the exact DOS, which is described by Eq. (37), but the linear combination of the exact DOS and the "smoothed" DOS [given by Eq. (31)], with the relative weights of $1/(1+b)$ and $b/(1+b)$, respectively. In order to reach the efficient elimination of the instrumental function one needs to choose the constant b as small as possible. In practice, the allowed compromise depends on the statistical accuracy of the experimental data. In our calculations we used $b=0.3$.

The calculated DOS for polycrystalline α-iron is shown in Fig. 2(a). It is compared to the data from neutron measurements[13] (solid line). Two sets of data show good agreement, however, our results do not reveal the sharp peak at $E=36$ meV. This discrepancy may be connected with the noncomplete elimination of the instrumental function and with the preliminary "smoothing" of the experimental data before the Fourier transformation.

Figures 2(b) and 2(c) show the projected densities of phonon states for the FeBO$_3$ single crystal, calculated for two nonequivalent crystallographic directions. The obvious difference in two PDOS confirms the anisotropy of phonon vibration in the ferric borate crystal, observed earlier in Ref. 9. According to Eq. (11), the peaks of PDOS correspond to the "high-density" areas in $\mathbf{q}$ space, where $|\mathrm{grad}_{\mathbf{q}}\hbar\omega_j(\mathbf{q})|$ is small for the particular branch j of the phonon modes. The conventional DOS includes the contributions of all branches, and all high-density areas contribute equally to DOS. In contrast to that, the contribution to PDOS is determined by the projection of the polarization vector $\mathbf{e}_{mj}(\mathbf{q})$ of the particular branch j to the direction $\mathbf{s}$ of the x-ray beam. Therefore high-density areas of various branches contribute differently to the projected density of states. Comparison of Figs. 2(b) and 2(c) shows that the phonons with the polarization vectors perpendicular to the [111] axis have one main high-density area in $\mathbf{q}$ space around the equienergetic surface of $E=22$ meV, whereas the phonons polarized along the [111] axis have at least two such areas, around $E=20$ meV and $E=30$ meV.

For each set of the experimental data the Lamb-Mössbauer factor was calculated. For α-iron we obtained $f_{\mathrm{LM}}=0.803\pm0.001$.[20] This agrees perfectly with the data of Ref. 6 and Ref. 7 (0.805 ± 0.003 and 0.803 ± 0.003, respectively). For the FeBO$_3$ crystal we obtained $f_{\mathrm{LM}}=0.837\pm0.003$ for the crystallographic direction, which has an angle of 85 ° to the [111] axes and $f_{\mathrm{LM}}=0.800\pm0.005$ for the direction along the [111] axes. This confirms the data obtained in the previous studies of lattice vibrations in the FeBO$_3$ crystal[9] (0.82 ± 0.02 and 0.81 ± 0.02, respectively).

Finally, we have calculated the mean sound velocity $\overline{c}$ for two considered crystallographic directions of the FeBO$_3$ crystal according to Eq. (45). For both directions we obtained $\overline{c}=(8\pm2)\times10^5$ cm/s. This value is close to the data reported in Ref. 21 [transversal modes sound velocity $c_t=(5\pm0.5)\times10^5$ cm/s, longitudinal mode $c_l=(9\pm1)\times10^5$ cm/s].

VII. SUMMARY

We have considered nuclear resonant inelastic absorption of x rays in the general case of the anisotropic single crystal. The derived expressions are similar to those of the Singwi and Sjölander theory[10] of nuclear absorption in the isotropic crystal. However, instead of the conventional DOS, the theory presented here deals with the projected density of phonon states, which is weighted by the projection of the phonon polarization vector to the direction of the x-ray beam.

We have described the method of calculation of PDOS from the experimental data, which is based on the forward and reversed Fourier transformations. The method provides the separation of the single-phonon absorption from the multiphonon contributions and deconvolution of the data with the instrumental function of the monochromator. Several useful relations between the energy moments of the experimental data with those of PDOS are derived, which allow one to verify the reliability of the obtained results.

In conclusion, we note that the developed theory is valid only for nuclear *absorption* experiment, where the yield of the products of nuclear internal conversion (atomic fluorescence or conversion electrons) is monitored. A theoretical description of the nuclear inelastic *scattering*, which considers the radiative channel of reemission of the incident x-ray photon, demands quite a different theoretical approach.

[1] A. K. Ghatak and L. S. Kothari, *An Introduction to Lattice Dynamics* (Addison-Wesley, London, 1972).

[2] R. W. James, *The Optical Principles of the Diffraction of X-Rays* (Ox Bow, Woodbridge, 1962).

[3] M. Cardona, in *Topics in Applied Physics Light Scattering in Solids II - Basic Concepts and Instrumentation*, edited by M. Cardona and G. Göntherodt (Springer-Verlag, Berlin, 1982), p. 19.

[4] E. Gerdau, R. Rüffer, H. Winkler, W. Tolksdorf, C. P. Klages, and J. P. Hannon, Phys. Rev. Lett. **54**, 853 (1985).

[5] M. Seto, Y. Yoda, S. Kikuta, X. W. Zhang, and M. Ando, Phys. Rev. Lett. **74**, 3828 (1995).

[6] W. Sturhahn, T. S. Toellner, E. E. Alp, X. Zhang, M. Ando, Y. Yoda, S. Kikuta, M. Seto, C. W. Kimball, and B. Dabrowski, Phys. Rev. Lett. **74**, 3832 (1995).

[7] A. I. Chumakov, R. Rüffer, A. Q. R. Baron, H. Grünsteudel, and H. F. Grünsteudel, Phys. Rev. B **54**, 9596 (1996).

[8] B. Fultz, C. C. Ahn, E. E. Alp, W. Sturhahn, and T. S. Toellner, Phys. Rev. Lett. **79**, 937 (1997).

[9] A. I. Chumakov, R. Rüffer, A. Q. R. Baron, H. Grünsteudel, H. F. Grünsteudel, and V. G. Kohn, Phys. Rev. B **56**, 10 758 (1997).

[10] K. S. Singwi and A. Sjölander, Phys. Rev. **120**, 1093 (1960).

[11] G. T. Trammell, Phys. Rev. **126**, 1045 (1962).

[12] H. J. Lipkin, Ann. Phys. (N.Y.) **18**, 182 (1962).

[13] H. R. Schober and P. H. Dederichs, in *Phonon States of Elements, Electron States and Fermi Surfaces of Alloys*, edited by K.-H. Hellwege and J. L. Olsen, Landolt-Börnstein, New Series, Group 3, Vol. 13, Pt. a (Springer, Berlin, 1981), p. 56.

[14] L. Van Hove, Phys. Rev. **95**, 249 (1954).

[15] Yu. Kagan, A. M. Afanas'ev, and V. G. Kohn, J. Phys. C **12**, 615 (1979).

[16] G. V. Smirnov and V. G. Kohn, Phys. Rev. B **52**, 3356 (1995).

[17] We note that the similar approach was used in T. S. Toellner, Ph.D. thesis, Northwestern University, 1996.

[18] R. Rüffer and A. I. Chumakov, Hyperfine Interact. **97-98**, 589 (1996).

[19] A. I. Chumakov, J. Metge, A. Q. R. Baron, H. Grünsteudel, H. N. Grünsteudel, R. Rüffer, and T. Ishikawa, Nucl. Instrum. Methods Phys. Res. A **383**, 642 (1996).

[20] For all these examples the indicated error was determined from the difference between the f_{LM} obtained from the area of the inelastic part of the probability density via Eq. (34) and from the calculated PDOS via Eq. (18). This gives the estimation of the statistical accuracy of the data. As for the systematical error, it is determined mostly by the precision of the alignment of the high-energy-resolution monochromator. We estimate this to be about 0.005 for all data sets.

[21] W. Jantz, J. R. Sandercock, and W. Wettling, J. Phys. C **9**, 2229 (1976).